

Table 3. Monthly Eurasian snow cover anomaly (in sq million km) (1967–1982)

Year	Months					
	Jan. (28.8)	Feb. (29.1)	Mar. (25.1)	Apr. (17.8)	May (10.8)	Jun. (4.8)
1967	-1.8	-1.7	-1.3	-3.0	-1.6	-0.3
1968	1.0	3.5	0.8	-2.3	-2.3	-0.2
1969	-2.8	-2.6	-1.7	1.4	1.2	-1.5
1970	-2.1	-4.6	-3.2	-0.3	-1.8	0.0
1971	-1.6	1.0	2.4	-0.8	1.6	0.8
1972	2.6	5.3	-0.3	0.9	0.4	-0.1
1973	1.5	2.1	0.8	1.1	1.4	0.3
1974	-0.2	0.1	1.3	1.3	0.8	3.2
1975	-1.1	-0.6	-0.1	-0.2	-0.5	0.6
1976	-0.9	0.2	2.3	1.1	3.5	2.9
1977	3.5	-0.7	1.6	1.2	1.7	-1.1
1978	3.4	4.8	2.4	-1.2	2.5	2.5
1979	3.9	2.2	2.4	3.0	1.7	0.2
1980	-0.8	1.8	2.5	4.1	2.0	2.0
1981	-3.4	-1.6	2.5	2.6	0.9	1.6
1982	0.5	-1.5	-1.0	-1.3	-2.1	-1.4
Drought yrs (5)	1.6	1.9	0.6	0.3	-0.3	0.3
Mean flood yrs (2)	-1.6	-2.6	-1.7	-0.3	-1.2	0.3
Normal yrs (9)	-0.3	0.3	1.3	0.6	1.4	0.7

The cold cyclonic anomalies during the drought years have an adverse effect on Indian summer monsoon. They can be responsible for more snow cover over Eurasia which subsequently can affect the Indian summer monsoon by delay of summer heating of land masses⁶.

Table 3 shows yearwise (1967–1982) snow cover anomaly during January to June. The mean value of each month is also given in brackets. The mean is calculated using the data of 24-year period, i.e. 1967–1990. It reveals that Eurasian snow cover was generally more than normal during the winter and premonsoon months of the drought years except 1982. Another conspicuous exception is the excess snow cover anomaly for the normal rainfall year 1978 which is very similar to the anomaly for drought year 1979.

In the study of Rajeevan², large upper tropospheric westerlies were observed over northwestern India during drought years. They are, in fact, associated with the cold anomalous cyclonic circulation reported in this study. The equatorial side of the cyclonic circulation brings cold dry air from west and northwest which may suppress organized convective activity.

1. Keshavamurty, R. N., Satyan, V., Dash, K. and Sinha, H. S. S., *Proc. Indian Acad. Sci. (Earth Planet. Sci.)* 1980, **89**, 209–214.
2. Rajeevan, M., *Mausam*, 1991, **42**, 155–160.
3. Verma, R. K., *Mausam*, 1982, **33**, 35–44.
4. Krishnamurti, T. N., Bedi, H. S. and Subramaniam, M., *J. Climatol.*, 1989, **2**, 321–340.
5. Parthasarathy, B., Sontakke, N. A., Monot, A. A. and Kothewale, D. A., *J. Climatol.*, 1987, **7**, 57–70.
6. Shukla, J., in *Monsoons* (eds. Fein, J. S. and Stephens, P. L.), 1987, pp. 399–463.

ACKNOWLEDGEMENTS. I thank Prof. R. N. Keshavamurty, Director, Indian Institute of Tropical Meteorology for his valuable guidance and for providing all the facilities to carry out the research at PRL, Ahmedabad. I also thank the Director General of Meteorology, Indian Meteorological Department for permitting submission of the paper to this journal and to the anonymous referees for their valuable comments and suggestions.

Received 23 April 1992; revised accepted 12 November 1992

Crystal structure of monochloro trinitro Cu(II) lignocaine complex

A. Indira, A. M. Babu, S. B. Bellad, M. A. Sridhar, J. Shashidhara Prasad and C. K. Prout*

Department of Studies in Physics, University of Mysore, Manasagangotri, Mysore 570 006, India

*Chemical Crystallography Laboratory, University of Oxford, 9, Parks Road, Oxford, OX1 3PD, UK

The crystal structure of monochloro trinitro copper (II) lignocaine complex, $\text{CuC}_{28}\text{H}_{44}\text{O}_{11}\text{N}_7\text{Cl}$, has been determined by X-ray diffraction using CuK_α radiation. The compound crystallizes in the monoclinic space group $P\bar{2}_1/n$ with unit cell parameters $a=10.554(2)$ Å, $b=24.402(7)$ Å, $c=14.124(3)$ Å, $\beta=100.025(20)^\circ$ with $Z=4$, $D_c=1.398 \text{ Mg m}^{-3}$, $D_m=1.391 \text{ Mg m}^{-3}$, $\mu=2.08 \text{ mm}^{-1}$. The structure was solved using 5242 reflections [$I>2.5\sigma(I)$] out of 6764 reflections using MULTAN. The final residuals are $R_f=0.120$ ($R_w=0.109$). The copper coordination is seven in the complex. The plane of one of the nitrate groups almost bisects the molecule.

LIGNOCaine hydrochloride metal complexes command a very wide interest owing to their importance in medical applications^{1–17}. The coordination property of ligands with nitrogen atoms has received modest attention in recent years. Generally the ligand group will be nitrogen bonded to the metal atom either directly or through hydrogen bonding^{18–25}. The present investigation was undertaken in order to get an insight into the activity of the complex. Of particular interest is the coordination around copper. Earlier reports^{26–33} have revealed the numerous possible geometries around the Cu(II) atom, which solely depend upon the type of donor atom linked to the acceptors. Crystal structure studies of complexes of lignocaine hydrochloride with various metals have been undertaken by us to get an insight into the activity of these substances. In this paper we report the structural study of the monochloro trinitro copper (II) lignocaine complex. We have earlier reported the structure of lignocaine tetrachlorocuprate complex³⁴.

Crystals suitable for single crystal X-ray diffraction work were obtained from ethanol. The crystals were of

green colour. A mixture of methylene iodide and xylene was used to measure the density of the sample by flotation technique. The cell dimensions obtained by Weissenberg camera were refined using 25 reflections in $40^\circ \leq 2\theta \leq 50^\circ$ on an Enraf Nonius diffractometer. 6764 counter intensities were measured by $\omega - 2\theta$ scan mode with $2\theta_{\max} = 140.3^\circ$ of which 5242 counter intensities were treated as observed with $I > 2.5\sigma(I)$. Lorentz and polarization corrections were applied. Intensities were not corrected for absorption by the crystal.

The structure was solved using MULTAN 80 (ref. 35). A first Fourier E-map revealed the metal atom, chlorine

atom, one nitrogen and one oxygen atom. Successive Fourier difference maps revealed all the remaining nonhydrogen atoms. Block diagonal least squares refinement was carried out with isotropic thermal parameters till the residual saturated at 0.23 using the LSTSQ-NRCVAX program³⁶. Anisotropic refinement was started at this stage and was stopped when the residual was 0.16. All the hydrogen atoms were generated using the CREDIT-NRCVAX program³⁶. Few more cycles of block diagonal least squares refinement with anisotropic thermal parameters for the non-hydrogens and isotropic parameters for the hydrogens converged to $R_f = 0.12$. The last least-squares cycle was

Table 1. Atomic parameters x, y, z and Biso of non-hydrogens

Atom	x	y	z	Biso
CuI	0.81327(13)	0.83242(5)	0.20441(9)	6.60(6)
ClI	0.68547(20)	0.79418(7)	0.30848(14)	5.60(9)
O1	0.6555 (10)	0.8684 (4)	0.0917 (6)	12.6(6)
O2	0.8411 (9)	0.8817 (5)	0.0825 (7)	15.0(7)
O3	0.6818 (12)	0.9000 (4)	-0.0283 (7)	15.31
O4	0.9738 (15)	0.9112 (8)	0.4123 (13)	25.79
O5	0.9705 (12)	0.8462 (7)	0.3331 (10)	20.86
O6	0.8609 (6)	0.90704(22)	0.2821 (4)	7.2 (3)
O7	0.9771 (10)	0.7649 (5)	0.1754 (7)	15.50
O8	0.8153 (8)	0.7612 (3)	0.1206 (6)	11.6 (5)
O9	0.9138 (15)	0.7117 (5)	0.0674 (10)	19.99
N1	0.7259 (9)	0.8825 (3)	0.0515 (5)	8.7 (5)
N2	0.9028 (6)	0.8953 (3)	0.3153 (5)	5.9 (3)
N3	0.8840 (7)	0.7543 (3)	0.1364 (6)	8.1 (4)
OL1	0.3653 (5)	0.68005(20)	0.0575 (4)	5.79(25)
OL2	0.4780 (6)	0.9690 (3)	0.4113 (4)	9.6 (4)
NL1	0.5183 (8)	0.7016 (3)	0.1843 (5)	7.7 (4)
NL2	0.3687 (7)	0.7776 (3)	-0.0259 (4)	5.8 (3)
NL3	0.5231 (6)	0.9092 (3)	0.3044 (5)	6.1 (3)
NL4	0.6663 (6)	0.9381 (3)	0.5521 (4)	5.8 (3)
C1	0.5423 (11)	0.5512 (4)	0.3230 (8)	8.8 (6)
C2	0.6126 (10)	0.5595 (4)	0.2537 (8)	9.0 (6)
C3	0.6074 (10)	0.6088 (4)	0.2050 (7)	8.1 (5)
C4	0.6872 (14)	0.6181 (6)	0.1286 (11)	12.1 (9)
C5	0.5248 (9)	0.6486 (3)	0.2326 (6)	6.5 (4)
C6	0.4505 (10)	0.6412 (4)	0.3020 (6)	7.4 (5)
C7	0.3678 (12)	0.6842 (5)	0.3306 (9)	10.1 (7)
C8	0.4636 (11)	0.5895 (4)	0.3490 (7)	8.5 (5)
C9	0.4394 (8)	0.7117 (3)	0.1011 (6)	6.1 (4)
C10	0.4449 (11)	0.7717 (4)	0.0687 (7)	9.2 (6)
C11	0.2561 (14)	0.8161 (5)	-0.0271 (10)	11.8 (8)
C12	0.1514 (14)	0.7942 (6)	0.0228 (10)	12.0 (9)
C13	0.9398 (13)	0.7014 (5)	0.3996 (8)	10.8 (8)
C14	1.0521 (17)	0.7469 (9)	0.3982 (12)	17.46
C15	0.1947 (12)	0.9454 (5)	0.1086 (8)	10.3 (7)
C16	0.3076 (13)	0.9725 (5)	0.0985 (7)	10.2 (7)
C17	0.4216 (9)	0.9597 (4)	0.1656 (6)	7.0 (5)
C18	0.5410 (13)	0.9887 (5)	0.1585 (9)	10.0 (7)
C19	0.4132 (8)	0.9221 (3)	0.2352 (5)	5.6 (4)
C20	0.2973 (10)	0.8932 (4)	0.2443 (7)	7.7 (5)
C21	0.2918 (12)	0.8516 (5)	0.3189 (8)	9.5 (7)
C22	0.1857 (9)	0.9085 (5)	0.1761 (8)	9.3 (6)
C23	0.5462 (8)	0.9344 (3)	0.3868 (6)	6.1 (4)
C24	0.6714 (9)	0.9184 (4)	0.4544 (6)	7.4 (5)
C25	0.6054 (16)	0.8926 (6)	0.6031 (10)	13.52
C26	0.5613 (16)	0.9011 (7)	0.6835 (12)	14.90
C27	0.7885 (11)	0.9554 (5)	0.6048 (9)	10.2 (6)
C28	0.8364 (12)	1.0053 (5)	0.5707 (12)	12.0 (9)

Biso is the mean of the principal axes of the thermal ellipsoid.
The last digit in each case is ESD.

calculated with 92 atoms, 561 parameters and 5232 out of 6764 reflections. Unit weights were used. The residuals for all reflections are $R_f = 0.120$, $R_w = 0.109$, where $R_f = \sum(F_o - F_c)/\sum(F_o)$, $R_w = [\sum(w(F_o - F_c)^2)/\sum(wF_o^2)]^{1/2}$. The maximum shift/sigma ratio was 0.865. In the last D-map, the deepest hole was $-0.760 \text{ e } \text{\AA}^{-3}$, and the highest peak was $0.740 \text{ e}/\text{\AA}^3$. The computational work was carried out on a ZENITH 386SX computer with a coprocessor. The final positional parameters, anisotropic thermal parameters for nonhydrogens, bond lengths and bond angles are given in Tables 1-4.

The bond lengths and angles are in good agreement with the standard values. The projection of the

molecule on the best plane is given in Figure 1. The bond lengths are slightly less than those found for the uranyl nitrate group in the complex of lignocaine hydrochloride-uranium nitrate³⁷. These values differ slightly from those quoted by Barclay *et al.*³⁸. The cell dimensions are almost equal to those of lignocaine tetrachlorocuprate complex³⁴. In view of the increased number of atoms for the same cell, the density of the crystal is slightly higher. The packing of the molecules down a and c is shown in Figures 2 and 3. The packing of the molecules also shows a similar arrangement to that seen in lignocaine tetrachlorocuprate complex³⁴. One interesting feature of the title compound is the

Table 2. $u(i,j)$ or U values *100 of non-hydrogens.

Atom	$u_{11}(U)$	u_{22}	u_{33}	u_{12}	u_{13}	u_{23}
CU1	8.81 (8)	7.42 (8)	9.48 (9)	-1.36 (7)	3.30 (7)	-2.58 (7)
CL1	9.11 (13)	5.14 (10)	6.88 (11)	-0.45 (9)	1.01 (10)	-0.42 (8)
O1	19.7 (9)	13.0 (7)	15.5 (8)	-4.2 (6)	4.2 (7)	-1.9 (6)
O2	15.9 (8)	27.9 (13)	14.4 (8)	-2.4 (8)	6.2 (7)	-3.7 (8)
O3	24.969	17.729	15.707	2.224	4.240	3.561
O4	25.471	40.437	34.617	-11.241	12.270	-12.119
O5	16.590	37.620	24.403	-7.022	1.757	2.483
O6	11.5 (5)	7.0 (4)	9.0 (4)	-0.3 (3)	1.7 (3)	-2.7 (3)
O7	16.077	27.235	16.210	4.733	4.612	0.501
O8	17.1 (7)	14.5 (7)	13.2 (6)	-7.5 (6)	4.6 (6)	-5.8 (5)
O9	36.234	16.939	27.377	-0.179	18.300	-5.319
N1	17.5 (8)	8.7 (5)	7.5 (5)	-0.6 (5)	3.9 (5)	2.9 (4)
N2	6.8 (4)	7.1 (4)	8.5 (4)	-1.9 (3)	1.4 (3)	-3.3 (3)
N3	8.5 (5)	9.2 (5)	12.1 (6)	2.0 (4)	-1.1 (5)	-3.6 (5)
OL1	8.8 (4)	5.5 (3)	6.9 (3)	-2.3 (3)	-1.0 (3)	0.54 (25)
OL2	11.9 (5)	13.3 (6)	9.5 (4)	8.4 (5)	-3.3 (4)	-6.4 (4)
NL1	11.8 (6)	7.4 (5)	8.2 (5)	-4.4 (4)	-3.0 (4)	2.4 (4)
NL2	9.8 (5)	6.1 (4)	5.9 (4)	-1.1 (4)	1.0 (3)	1.4 (3)
NL3	7.0 (4)	8.8 (5)	7.2 (4)	2.2 (4)	0.7 (3)	-3.0 (4)
NL4	8.3 (4)	6.8 (4)	6.3 (4)	2.5 (3)	-0.2 (3)	-0.9 (3)
C1	12.1 (8)	8.1 (7)	11.9 (8)	0.2 (6)	-1.6 (7)	3.0 (6)
C2	10.1 (8)	9.0 (7)	13.8 (9)	0.6 (6)	-1.9 (7)	-0.2 (7)
C3	9.1 (7)	9.4 (7)	11.2 (8)	-2.2 (6)	-1.3 (6)	0.9 (6)
C4	14.9 (12)	14.9 (12)	17.2 (13)	-2.7 (9)	5.3 (10)	-0.5 (10)
C5	10.0 (6)	6.4 (5)	6.8 (5)	-2.3 (5)	-2.4 (4)	1.0 (4)
C6	12.0 (8)	7.3 (6)	7.9 (6)	-1.7 (5)	-0.5 (5)	0.4 (5)
C7	12.5 (9)	11.6 (9)	14.3 (10)	2.1 (7)	2.2 (8)	-1.0 (8)
C8	13.7 (9)	9.7 (7)	8.2 (6)	-2.4 (6)	-0.2 (6)	2.9 (5)
C9	7.9 (5)	6.8 (5)	7.9 (5)	-2.0 (4)	0.1 (4)	2.4 (4)
C10	15.0 (10)	7.5 (6)	10.5 (7)	-4.8 (6)	-3.0 (7)	3.2 (5)
C11	18.6 (13)	8.5 (8)	16.4 (12)	1.0 (8)	-0.7 (10)	-4.4 (8)
C12	15.5 (12)	16.3 (12)	15.3 (11)	-2.2 (10)	6.0 (9)	-5.9 (10)
C13	17.9 (12)	13.3 (10)	10.7 (8)	-6.6 (9)	4.6 (8)	0.4 (7)
C14	18.748	29.446	18.261	-10.317	3.533	-7.665
C15	13.4 (9)	15.5 (11)	8.9 (7)	6.5 (8)	-1.1 (7)	-3.7 (7)
C16	19.5 (13)	12.1 (9)	7.0 (6)	4.9 (9)	1.4 (7)	-1.0 (6)
C17	10.7 (7)	9.0 (6)	7.3 (5)	1.5 (5)	2.1 (5)	-1.6 (5)
C18	15.8 (11)	10.6 (8)	12.8 (9)	-1.3 (8)	5.6 (8)	0.5 (7)
C19	7.2 (5)	7.9 (5)	6.1 (4)	1.1 (4)	0.9 (4)	-2.2 (4)
C20	10.6 (7)	10.0 (7)	8.4 (6)	1.2 (6)	1.1 (5)	-4.4 (5)
C21	13.3 (9)	10.3 (8)	12.9 (9)	-3.2 (7)	3.4 (8)	-0.2 (7)
C22	7.0 (6)	16.1 (11)	11.7 (8)	1.2 (6)	0.2 (6)	-5.7 (8)
C23	7.2 (5)	8.5 (6)	6.9 (5)	2.5 (4)	-0.1 (4)	-2.2 (4)
C24	8.7 (6)	11.3 (7)	7.5 (5)	4.0 (5)	-0.6 (5)	-3.7 (5)
C25	23.983	14.398	15.560	10.822	10.611	5.417
C26	17.559	21.529	19.779	3.815	9.484	2.670
C27	10.7 (8)	11.8 (9)	14.3 (10)	3.9 (7)	-3.4 (7)	-5.4 (8)
C28	11.7 (10)	10.1 (9)	23.7 (16)	0.7 (7)	2.6 (10)	0.1 (10)

Anisotropic temperature factors are of the form, Temp. = $-2 \cdot P_i \cdot P_j \cdot (h \cdot h \cdot u_{11} + a \cdot a \cdot u_{12} + \dots + 2 \cdot h \cdot k \cdot u_{12} \cdot a \cdot a + \dots)$
The last digit in each case is ESD.

Table 3. Bond lengths of non-hydrogens

Cu(1)-Cl(1)	2.3538(24)	NL(4)-C(27)	1.437(12)
Cu(1)-O(2)	2.161(11)	C(1)-C(2)	1.342(18)
Cu(1)-O(6)	2.140(5)	C(1)-C(8)	1.344(17)
Cu(1)-O(8)	2.105(7)	C(2)-C(3)	1.380(15)
O(1)-N(1)	1.067(12)	C(3)-C(4)	1.498(18)
O(2)-N(1)	1.218(14)	C(3)-C(5)	1.405(15)
O(3)-N(1)	1.219(12)	C(5)-C(6)	1.370(14)
O(4)-N(2)	1.495(18)	C(6)-C(7)	1.466(15)
O(5)-N(2)	1.395(18)	C(6)-C(8)	1.421(13)
O(6)-N(2)	0.652(9)	C(9)-C(10)	1.540(11)
O(7)-O(8)	1.750(13)	C(11)-C(12)	1.508(21)
O(7)-N(3)	1.071(13)	C(13)-NL(2) ^b	1.486(14)
O(8)-N(3)	0.739(12)	C(13)-C(14)	1.627(20)
O(9)-N(3)	1.497(13)	C(15)-C(16)	1.392(21)
OL(1)-C(9)	1.191(9)	C(15)-C(22)	1.327(19)
OL(2)-C(23)	1.199(9)	C(16)-C(17)	1.431(15)
NL(1)-C(5)	1.457(10)	C(17)-C(18)	1.463(16)
NL(1)-C(9)	1.339(10)	C(17)-C(19)	1.359(13)
NL(2)-C(10)	1.441(11)	C(19)-C(20)	1.437(14)
NL(2)-C(11)	1.513(15)	C(20)-C(21)	1.471(16)
NL(2)-C(13) ^a	1.486(14)	C(20)-C(22)	1.434(14)
NL(3)-C(19)	1.416(10)	C(23)-C(24)	1.540(11)
NL(3)-C(23)	1.301(9)	C(25)-C(26)	1.316(19)
NL(4)-C(24)	1.471(10)	C(27)-C(28)	1.432(19)
NL(4)-C(25)	1.525(16)		

The last digit in each case is ESD.

seven coordination, i.e. with six oxygens of the three nitrate groups and one chlorine atom. Such high coordination is observed to give rise to a distorted pentagonal-bipyramidal environment. This is evident

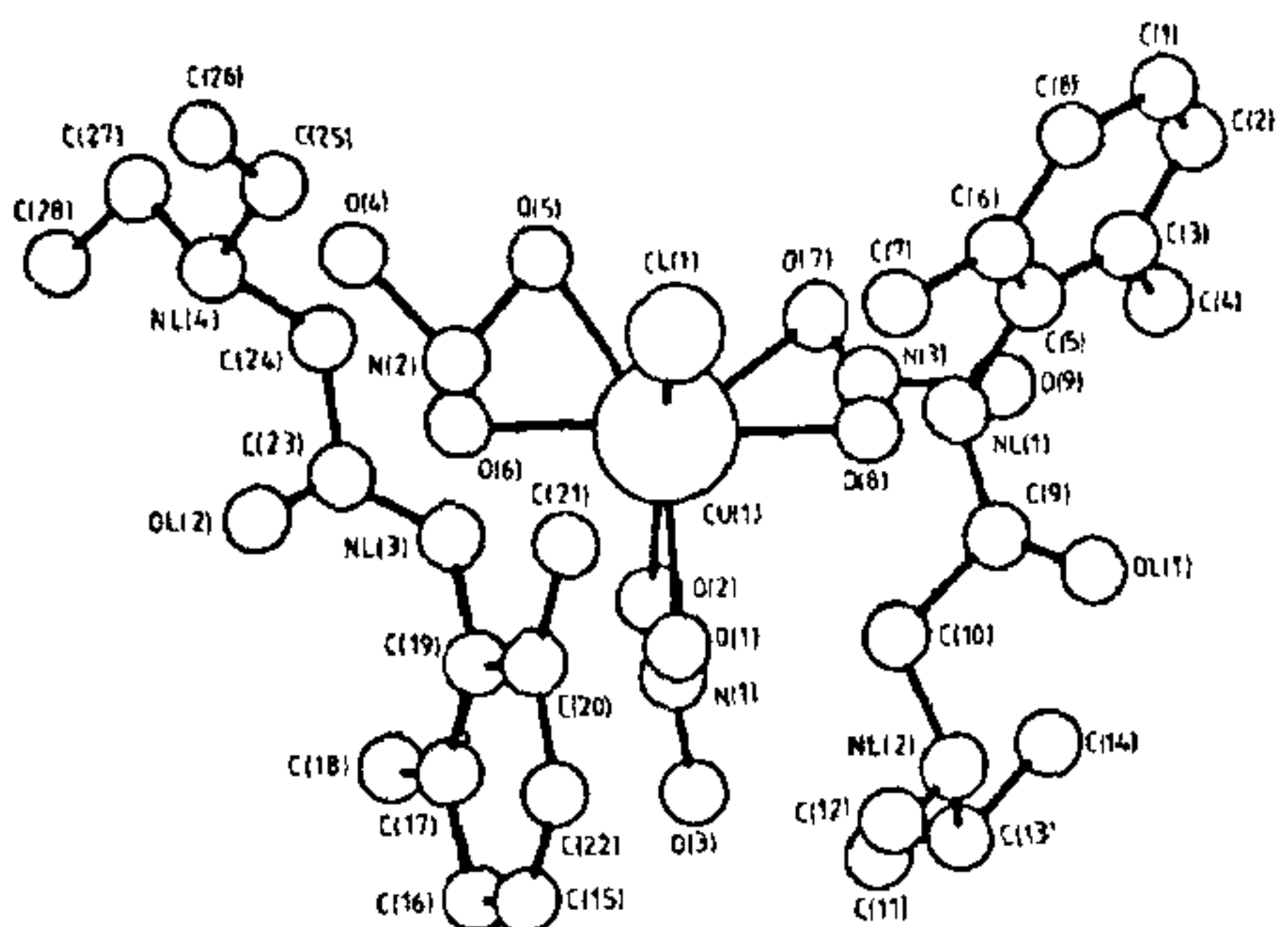


Figure 1. Projection of the molecule on the best plane.

from the least-squares planes data for the metal group given in Table 5 (refs. 39, 40). Some of the bond lengths and angles of this group are given in Table 6. The relatively large thermal parameters of the terminal oxygens of the nitrate groups can be due to the stacking considerations of the distorted pentagonal-bipyramidal in between the two layers of the ligand. The distribution of the ligands about the central metal atom appears as

Table 4. Bond angles of non-hydrogens

Cl(1)-Cu(1)-O(2)	152.9(3)	C(4)-C(3)-C(5)	123.3(9)
Cl(1)-Cu(1)-O(6)	97.26(18)	NL(1)-C(5)-C(3)	117.7(8)
Cl(1)-Cu(1)-O(8)	94.98(22)	NL(1)-C(5)-C(6)	117.8(9)
O(2)-Cu(1)-O(6)	83.3(3)	C(3)-C(5)-C(6)	124.5(8)
O(2)-Cu(1)-O(8)	89.7(4)	C(5)-C(6)-C(7)	123.0(9)
O(6)-Cu(1)-O(8)	165.1(3)	C(5)-C(6)-C(8)	115.5(9)
Cu(1)-O(2)-N(1)	91.8(6)	C(7)-C(6)-C(8)	121.4(10)
Cu(1)-O(6)-N(2)	93.6(7)	C(1)-C(8)-C(6)	120.3(10)
O(8)-O(7)-N(3)	12.3(5)	OL(1)-C(9)-NL(1)	125.9(7)
Cu(1)-O(8)-O(7)	79.3(5)	OL(1)-C(9)-C(10)	121.2(7)
Cu(1)-O(8)-N(3)	97.1(8)	NL(1)-C(9)-C(10)	112.8(7)
O(7)-O(8)-N(3)	17.9(7)	NL(2)-C(10)-C(9)	109.1(7)
O(1)-N(1)-O(2)	123.1(9)	NL(2)-C(11)-C(12)	114.4(10)
O(1)-N(1)-O(3)	114.6(11)	NL(2)b-C(13)-C(14)	103.4(10)
O(2)-N(1)-O(3)	122.4(10)	C(16)-C(15)-C(22)	124.4(10)
O(4)-N(2)-O(5)	84.2(10)	C(15)-C(16)-C(17)	117.7(10)
O(4)-N(2)-O(6)	135.5(11)	C(16)-C(17)-C(18)	118.9(10)
O(5)-N(2)-O(6)	140.3(10)	C(16)-C(17)-C(19)	118.2(10)
O(7)-N(3)-O(8)	149.8(12)	C(18)-C(17)-C(19)	122.8(9)
O(7)-N(3)-O(9)	102.9(10)	NL(3)-C(19)-C(17)	120.0(8)
O(8)-N(3)-O(9)	105.5(11)	NL(3)-C(19)-C(20)	115.9(8)
C(5)-NL(1)-C(9)	123.0(6)	C(17)-C(19)-C(20)	124.0(8)
C(10)-NL(2)-C(11)	112.5(8)	C(19)-C(20)-C(21)	122.8(9)
C(10)-NL(2)-C(13) ^a	114.9(8)	C(19)-C(20)-C(22)	115.1(10)
C(11)-NL(2)-C(13) ^a	105.7(8)	C(21)-C(20)-C(22)	122.0(10)
C(19)-NL(3)-C(23)	121.1(6)	C(15)-C(22)-C(20)	120.4(10)
C(24)-NL(4)-C(25)	107.0(8)	OL(2)-C(23)-NL(3)	124.2(7)
C(24)-NL(4)-C(27)	113.9(8)	OL(2)-C(23)-C(24)	119.6(7)
C(25)-NL(4)-C(27)	112.6(9)	NL(3)-C(23)-C(24)	116.2(6)
C(2)-C(1)-C(8)	122.6(9)	NL(4)-C(24)-C(23)	109.3(6)
C(1)-C(2)-C(3)	121.1(10)	NL(4)-C(25)-C(26)	122.3(13)
C(2)-C(3)-C(4)	120.8(11)	NL(4)-C(27)-C(28)	114.4(10)
C(2)-C(3)-C(5)	159.9(10)		

The last digit in each case is ESD.

Table 5. Least-squares planes data for the metal atom along with the three nitrate groups and chlorine atom (δx is the displacement from the 1.s plane in Å)

Atom	Plane 1 δx	Atom	Plane 2 δx	Atom	Plane 3 δx	Atom	Plane 4 δx
CU1	-0.0015(19)	CU1	-0.0010(19)	CU1	0.0011(19)	CU1	-0.0023(19)
O1	0.087 (13)	O4	-0.248 (21)	O7	-0.019 (17)	CL1	0.001 (3)
O2	0.112 (15)	O5	0.168 (20)	O8	-0.040 (11)	O1	0.055 (12)
O3	-0.1520(15)	O6	0.025 (9)	O9	0.226 (18)	O2	0.160 (13)
N1	0.019 (11)	N2	0.003 (8)	N3	-0.064 (10)	O3	-0.140 (15)
						N1	0.027 (11)

Dihedral angles (°) between the planes

Plane 1-plane 2	100.5(5)	Plane 2-plane 3	36.4 (6)
Plane 1-plane 3	85.6(3)	Plane 2-plane 4	98.34(21)
Plane 1-plane 4	2.3(5)	Plane 3-plane 4	84.17(21)

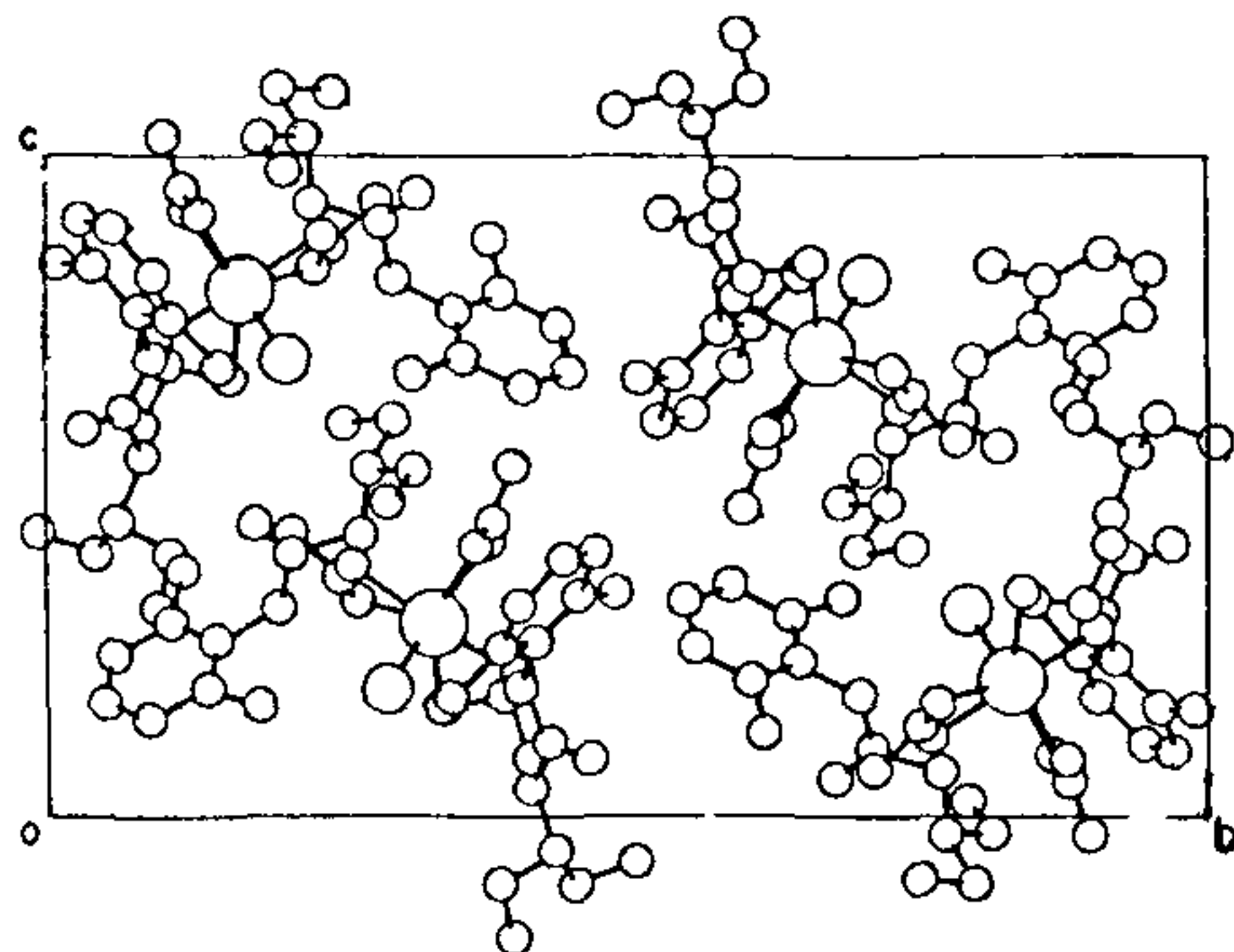


Figure 2. Packing of the molecules down *a*.

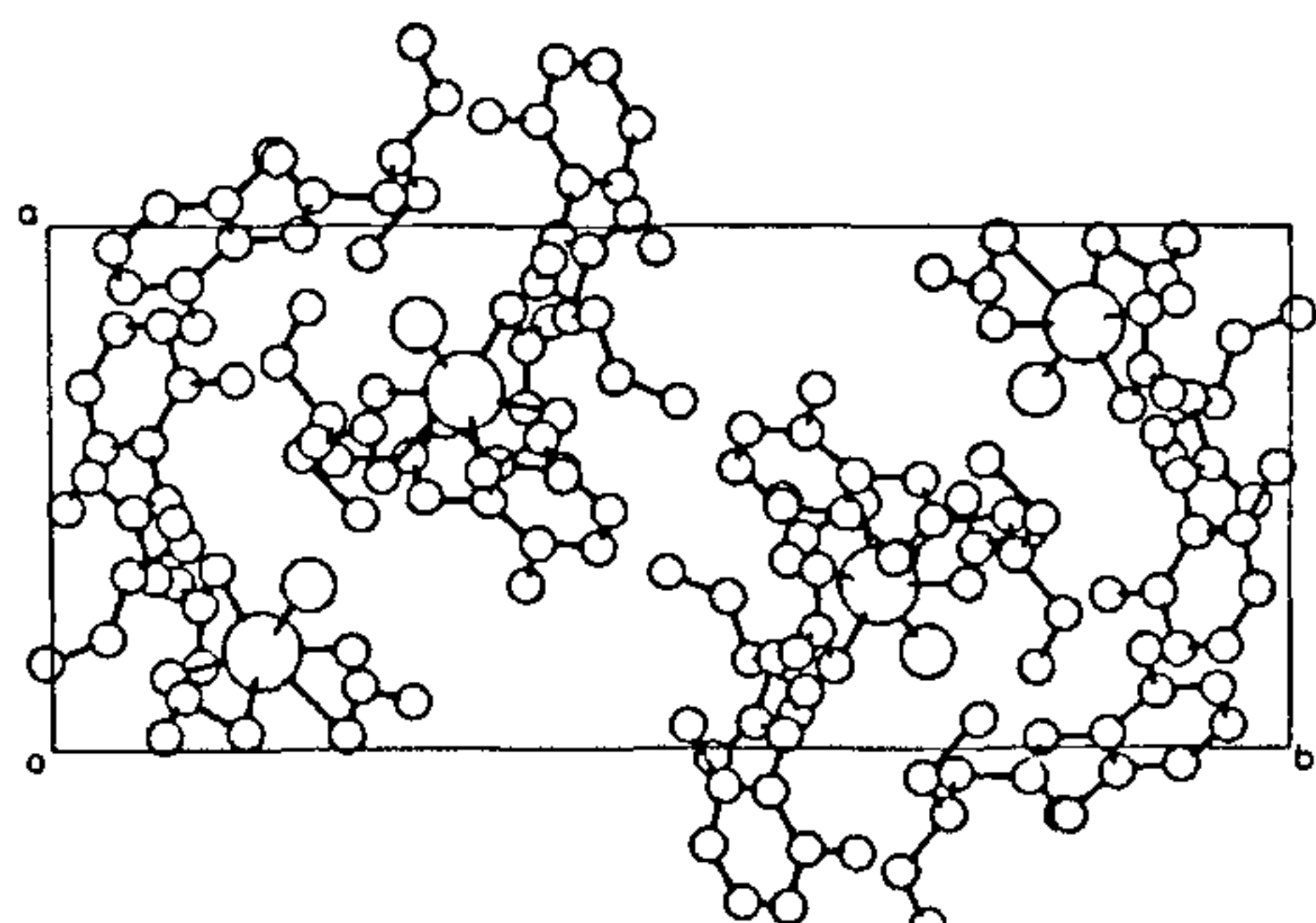


Figure 3. Packing of the molecules down *c*.

though the copper atom acts as an inversion centre. This can be seen even in the packing of the molecules along the three axes. The ligands are bound through

Table 6. Selected bond distances and bond angles of the metal group

Atom 1-Atom 2	Bond distances (Å)
Cu(1)-Cl(1)	2.3538(24)
Cu(1)-O(1)	2.270(10)
Cu(1)-O(2)	2.161(11)
Cu(1)-O(5)	2.262(12)
Cu(1)-O(6)	2.140(5)
Cu(1)-O(7)	2.474(10)
Cu(1)-O(8)	2.105(7)
O(1)-O(2)	2.011(14)
O(1)-N(1)	1.067(12)
O(2)-N(1)	1.218(14)
O(3)-N(1)	1.219(12)
O(4)-N(2)	1.495(18)
O(5)-O(6)	1.942(17)
O(6)-N(2)	0.652(9)
O(5)-N(2)	1.395(18)
O(7)-N(3)	1.071(13)
O(7)-O(8)	1.750(13)
O(1)-O(3)	1.926(13)
O(9)-N(3)	1.497(13)
O(1)-O(8)	3.100(14)
O(2)-O(6)	2.857(11)
O(5)-O(7)	2.992(19)

Atom 1-Atom 2-Atom 3	Bond angle (°)
O(1)-Cu(1)-O(2)	53.9(4)
O(1)-N(1)-O(2)	123.1(9)
O(1)-N(1)-O(3)	114.6(11)
O(2)-N(1)-O(3)	122.4(10)
O(5)-Cu(1)-O(6)	52.3(5)
O(4)-N(2)-O(5)	84.2(10)
O(5)-N(2)-O(6)	140.3(10)
O(4)-N(2)-O(6)	135.5(11)
O(7)-Cu(1)-O(8)	44.0(4)
O(7)-N(3)-O(8)	149.8(12)
O(8)-N(3)-O(9)	105.5(11)
O(7)-N(3)-O(9)	102.9(10)

The last digit in each case is FSD.

the chlorine atom according to the scheme NL(1)-H(10)...Cl(1)...H(32) NL(3). The bond distances of this scheme are 1.098 Å, 2.102 Å, 2.300 Å and 1.031 Å respectively.

1. Tosaki, A., Balint, S. and Szekeres, L., *J. Cardiovasc. Pharmacol.*, 1988, **12**, 621–628.
2. Clarkson, C. W., Follmer, C. H., TenEick, R. E., Hondeghem, L. M. V. and Yeh, J. Z., *Circ. Res.*, 1988, **63**, 869–878.
3. Zivanovic, L., Zivanov-Stakic, D. and Radulovic, D., *J. Pharm. Biomed. Anal.*, 1988, **6**, 809–812.
4. Blyden, G. T., Greenblatt, D. J., LeDuc, B. W. and Scavone, J. M., *Eur J. Clin. Pharmacol.*, 1988, **35**, 413–417.
5. DeLangen, C. D. J., Balke, C. W., Spear, J. F., Levine, J. H. and Moore, E. N., *J. Cardiovasc. Pharmacol.*, 1988, **12**, 683–688.
6. Onuaguluchi, G. and Igbo, I. N. A., *Arch. Int. Pharmacodyn. Ther.*, 1985, **274**, 253–266.
7. Martins, J. B. and Kelly, K. J., *Am. Heart J.*, 1985, **109**, 533–539.
8. Hinton, R. J., Dechow, P. C. and Carlson, D. S., *Oral Surg., Oral Med. Oral Pathol.*, 1985, **59**, 247–251.
9. Merrifield, A. J. and Carter, S. J., *Anaesthesia*, 1965, **20**, 287–289.
10. Hargrove, R. L., Hoyle, J. R., Parker, J. B. R., Beckett, A. H. and Boyes, R. N., *Anaesthesia*, 1966, **21**, 37–40.
11. Foldes, F. F., Molly, R., McNall, P. G. and Koukal, L. R., *J. Am. Med. Assoc.*, 1960, **172**, 1493–1498.
12. Bromage, P. R. and Robson, J. G., *Anaesthesia*, 1961, **16**, 461–463.
13. Ritchie, J. M. and Ritchie, B. R., *Science*, 1968, **162**, 1394–1395.
14. Buchie, J. and Perlia, X., *Arzneim-Forsch.*, 1962, **10**, 1–8, 117–124, 174–177, 297–301, 456–467, 554–559.
15. Ritchie, J. M. and Greengard, P., *Annu. Rev. Pharmacol.*, 1966, **6**, 405–409.
16. Thorsteinn, L., Masaaki, M., Caldwell, R. W., Gildersleeve, N. and Bodor, N., *Int. J. Pharm.*, 1984, **22**, 345–355.
17. Prippenow, G., Fruhstorfer, H., Seiditz, P. and Nolte, H., *Reg. Anaesth. (Berlin)*, 1985, **8**, 15–20.
18. Pajunen, A., *Acta Crystallogr.*, 1982, **B38**, 928–929.
19. Gutkosa, R., Lyford, P. and Zubietta, J. A., *Cryst. Struct. Commun.*, 1982, **11**, 1311–1316.
20. Abello, L., Ensuque, A., Demaret, A. and Lapluye, G., *Transition Met. Chem.*, 1980, **5**, 120–121.
21. Pavelcik, F. and Majer, J., *Acta Crystallogr.*, 1980, **B36**, 1645–1646.
22. Anan'eva, N. N., Polyakova, I. N., Polynova, T. N. and Porai-Koshits, M. A., *Koord. Khim.*, 1981, **7**, 1578–1584.
23. Petrovic, D., Leovac, V. M. and Lazar, D., *Cryst. Struct. Commun.*, 1981, **10**, 823–826.
24. Bertrand, J. A., Fujita, E. and Van Derveer, D. G., *Inorg. Chem.*, 1980, **19**, 2022–2028.
25. Cameron, A. F., Taylor, D. W. and Nuttall, R. H., *J. Chem. Soc. Dalton Trans.*, 1972, **15**, 1603–1608.
26. Coetzer, J., *Acta Crystallogr.*, 1970, **B26**, 1414–1417.
27. Pabst, I. and Bats, J. W., *Acta Crystallogr.*, 1985, **C41**, 1297–1299.
28. Saha, C. R., Sen, D. and Guha, S., *J. Chem. Soc. Dalton Trans.*, 1975, **16**, 1701–1706.
29. Stephens, F. S. and Tucker, P. A., *J. Chem. Soc. Dalton Trans.*, 1973, **21**, 2293–2297.
30. Matsumoto, K., Ooi, S., Nakasuka, K., Mori, W., Suzuki, S., Nakahara, A. and Nako, Y., *J. Chem. Soc. Dalton Trans.*, 1985, **10**, 2095–2100.
31. Bailey, N. A., Mckenzi, E. D. and Worthington, J. M., *J. Chem. Soc. Dalton Trans.*, 1973, **11**, 1227–1231.
32. Bertini, I., Dapporto, P., Gatteschi, D. and Scozzafava, A., *J. Chem. Soc. Dalton Trans.*, 1979, **9**, 1409–1414.
33. Xinmin, G., Ning, T., Xin, W., Yin, Z. and Minyu, T., *Polyhedron*, 1989, **8**, 933–935.
34. Srividhar, M. A., Babu, A. M., Indira, A., Bellad, S. B., Shashidhara Prasad, J., Ramappa, P. G. and Nagendrapappa, G., *Z. Kristallogr.*, 1992, **202**, 292–295.
35. Germain, G., Main, P. and Woolfson, M. M., *Acta Crystallogr.*, 1971, **A27**, 368–378.
36. Gabe, E. J., Le Page, Y., Charland, J. P., Lee, F. L. and White, P., *S. J. Appl. Crystallogr.*, 1989, **22**, 384–387.
37. Bellad, S. B., Indira, A., Srividhar, M. A., Babu, A. M., Shashidhara Prasad, J. and Prout, C. K., communicated.
38. Barclay, G. A., Sabine, T. M. and Taylor, J. C., *Acta Crystallogr.*, 1965, **19**, 205–209.
39. Drew, M. G. B., Nelson, J. and Nelson, S. M., *J. Chem. Soc., Dalton Trans.*, 1981, **8**, 1685–1690.
40. Palenik, G. J., Koziol, A. E., Gawron, M., Palenik, R. C. and Wester, D. W., *Acta Crystallogr.*, 1988, **C44**, 85–88.

ACKNOWLEDGEMENTS. We (A.L., A.M.B., S.B.B. and M.A.S.) thank UGC, New Delhi for financial assistance. We also thank Professor P. G. Ramappa, Department of Studies in Chemistry, University of Mysore, Mysore for kindly providing the sample. J.S.P. thanks DST, New Delhi for the financial assistance under the project No. SP/S2/M-34, 86.

Received 14 August 1992; revised accepted 23 November 1992

Visualization of three-dimensional data by 'volume rendering'

N. RAMESH and G. ATHITHAN

Advanced Numerical Research and Analysis Group,
P. O. Kanchanbagh, Hyderabad 500 258, India

We report an implementation of a ray-tracing method for visualizing volumetric data. For evaluating the performance of the implementation, we consider the visualization of two classes of volumetric data. The first consists of the probability density functions of a subset of states of an electron in hydrogen atom and represents the ease of visualizing data derived from analytical expressions. The second class of volumetric data is a set of three-dimensional fractals which are generated over regular three-dimensional cartesian grids of various sizes. The motivation for generating and visualizing the fractal data sets is two-fold. Firstly a fractal data set is a good test input to verify the correctness of the implementation. Secondly, we want to model stellar clouds and see how they can be visualized. Clouds are known to be akin to fractal data sets and we find that the volume rendered images of these data sets bear a close resemblance to stellar clouds. Ray-tracing is computationally expensive and we therefore report the CPU timings for a representative set of images. General comments on the utility of this method for visualizing in various disciplines conclude the paper.

REPRESENTATION and visualization of data in a graphical form is a practice as old as experimental science. Whether it is an array of numbers or a mathematical function, a graphical plot of the same gives better insight. However, before the advent of computer graphics, one was limited to visualizing the relationship between just two variables in a graphical form. Visualization of any relationship among three variables usually called for highly skilled draftsmen and that among four variables was out of the question. With the application of computer graphics, the problem of visua-